

Supporting information for:

Analysis of the Limits of the Near-Field

Produced by Nanoparticle Arrays

Alejandro Manjavacas,* Lauren Zundel, and Stephen Sanders

Department of Physics and Astronomy, University of New Mexico, Albuquerque, New Mexico 87131, United States

E-mail: manjavacas@unm.edu

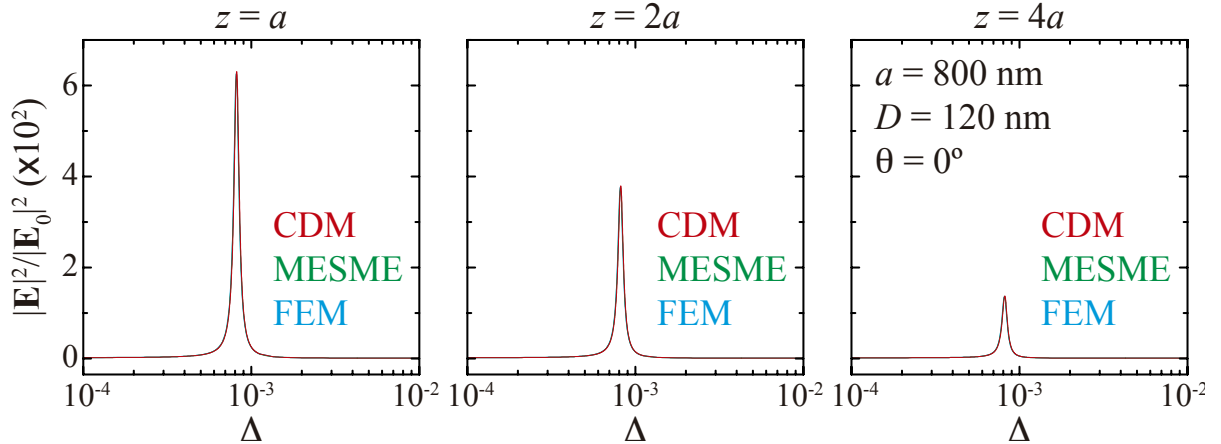


Figure S1: Comparison of the coupled dipole model (CDM) approach (red curves) with rigorous solutions of Maxwell's equations obtained using both a multiple elastic scattering of multipolar expansions (MESME) approach (green curves) and a finite element method (FEM) approach (blue curves). The plots show the enhancement of the field intensity, averaged over the unit cell, and calculated at different distances z above the array. In all cases, we consider an array of silver nanospheres with diameter $D = 120$ nm and period $a = 800$ nm, illuminated at normal incidence.

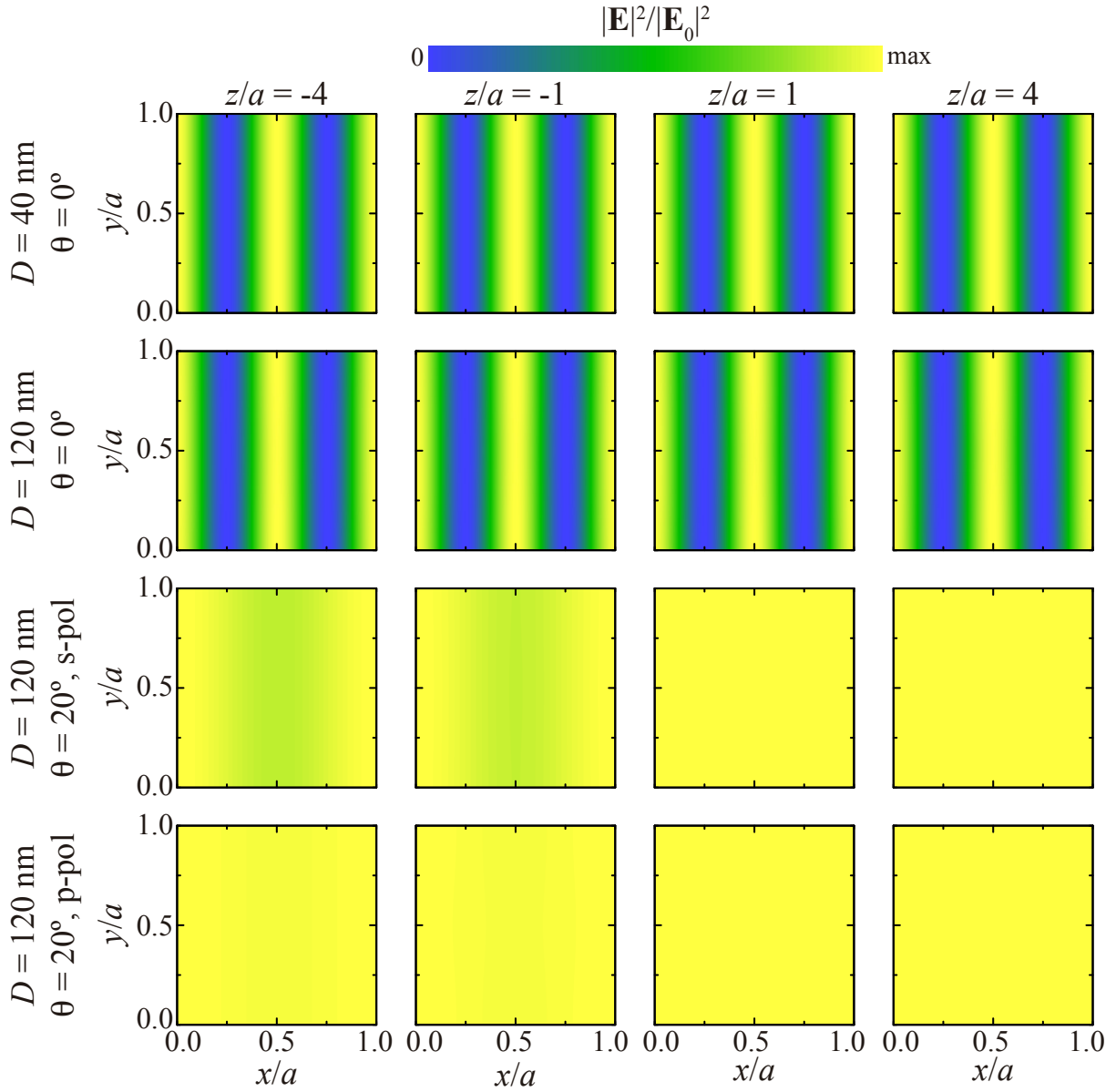


Figure S2: In-plane spatial dependence of the near-field intensity enhancement produced by different arrays. As indicated in the labels, we consider arrays composed of nanospheres of different diameters D , illuminated with light propagating at different angles θ and polarizations, and calculate the field intensity enhancement at different distances above and below the array. In all cases, the period of the array is $a = 800$ nm, and the results are normalized to the maximum value of the field intensity enhancement.

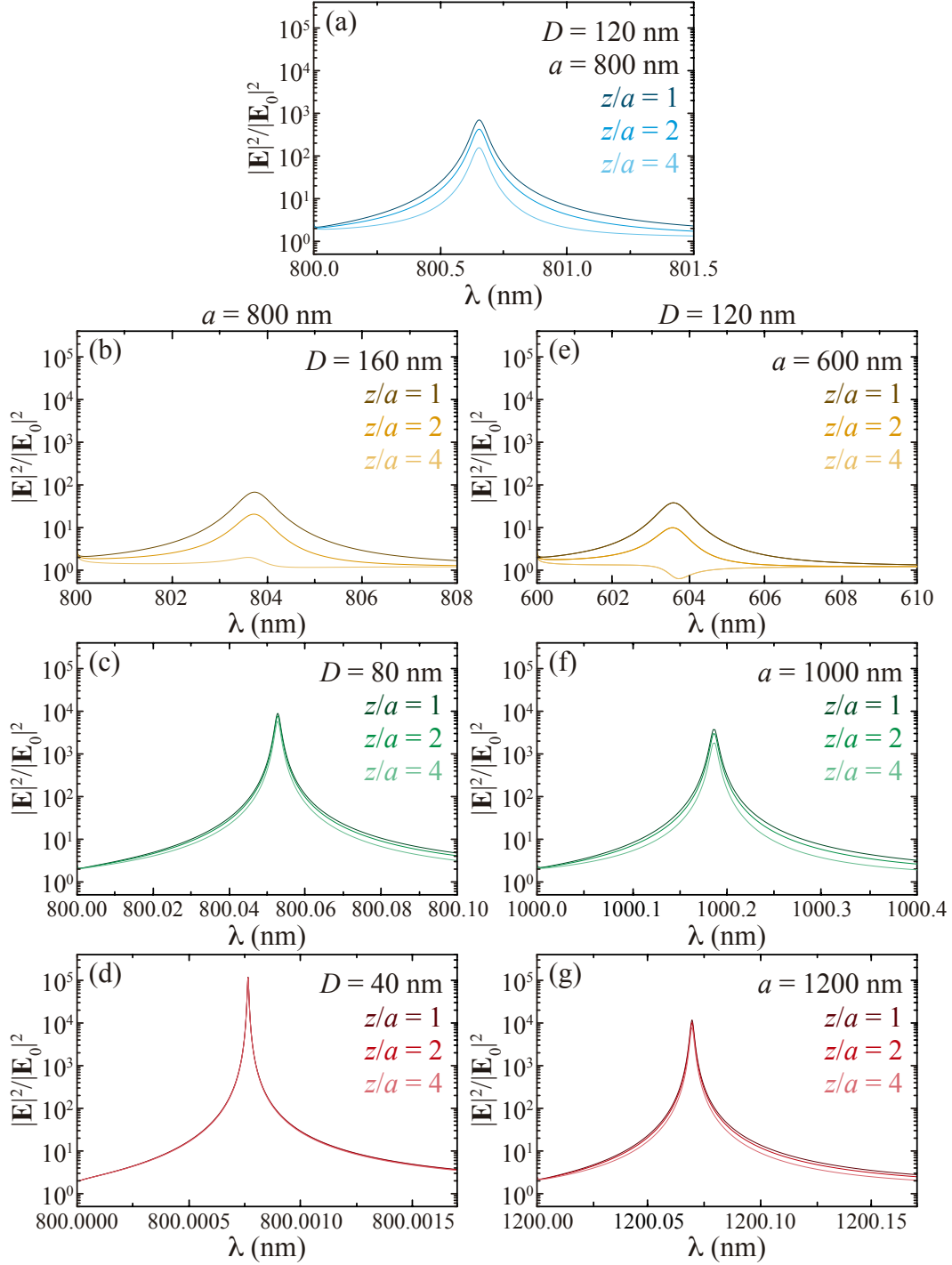


Figure S3: Plot of the near-field intensity enhancement of all cases from Figure 2(a) and (c) of the main paper, but as a function of λ rather than Δ . (a) Plot for $D = 120$ nm, $a = 800$ nm. (b-d) Plot for a constant periodicity $a = 800$ nm and diameters $D = 160$ nm (b), $D = 80$ nm (c), and $D = 40$ nm (d). (e-g) Plots for a constant diameter of $D = 120$ nm and periodicity $a = 600$ nm (e), $a = 1000$ nm (f), and $a = 1200$ nm (g). In all panels, the shade of the curve color indicates the distance from the array, as indicated by the legend.

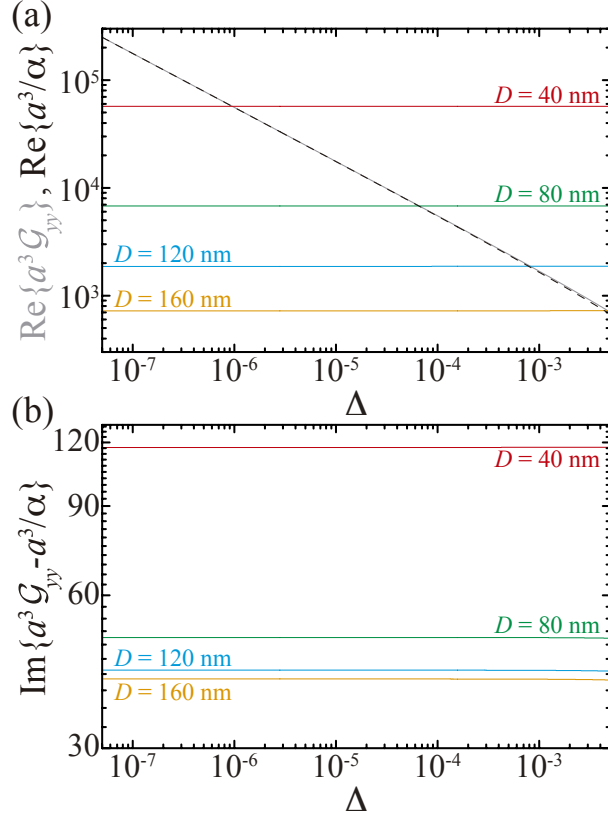


Figure S4: Analysis of the mechanism determining the linewidth of the lattice resonances. (a) Real part of the inverse of the polarizability for particles with different diameters (color curves) compared with the real part of the in-plane component of the lattice sum (gray curve). The black dashed curve represents the approximate value of $\text{Re}\{a^3 \mathcal{G}_{yy}(0)\} \approx 4\sqrt{2}\pi^2 \Delta^{-1/2} - 118$.^{S1,S2} (b) Imaginary part of the difference between the in-plane component of the lattice sum and the inverse of the particle polarizability for the same nanoparticles as in panel (a). In all cases, we assume $a = 800$ nm.

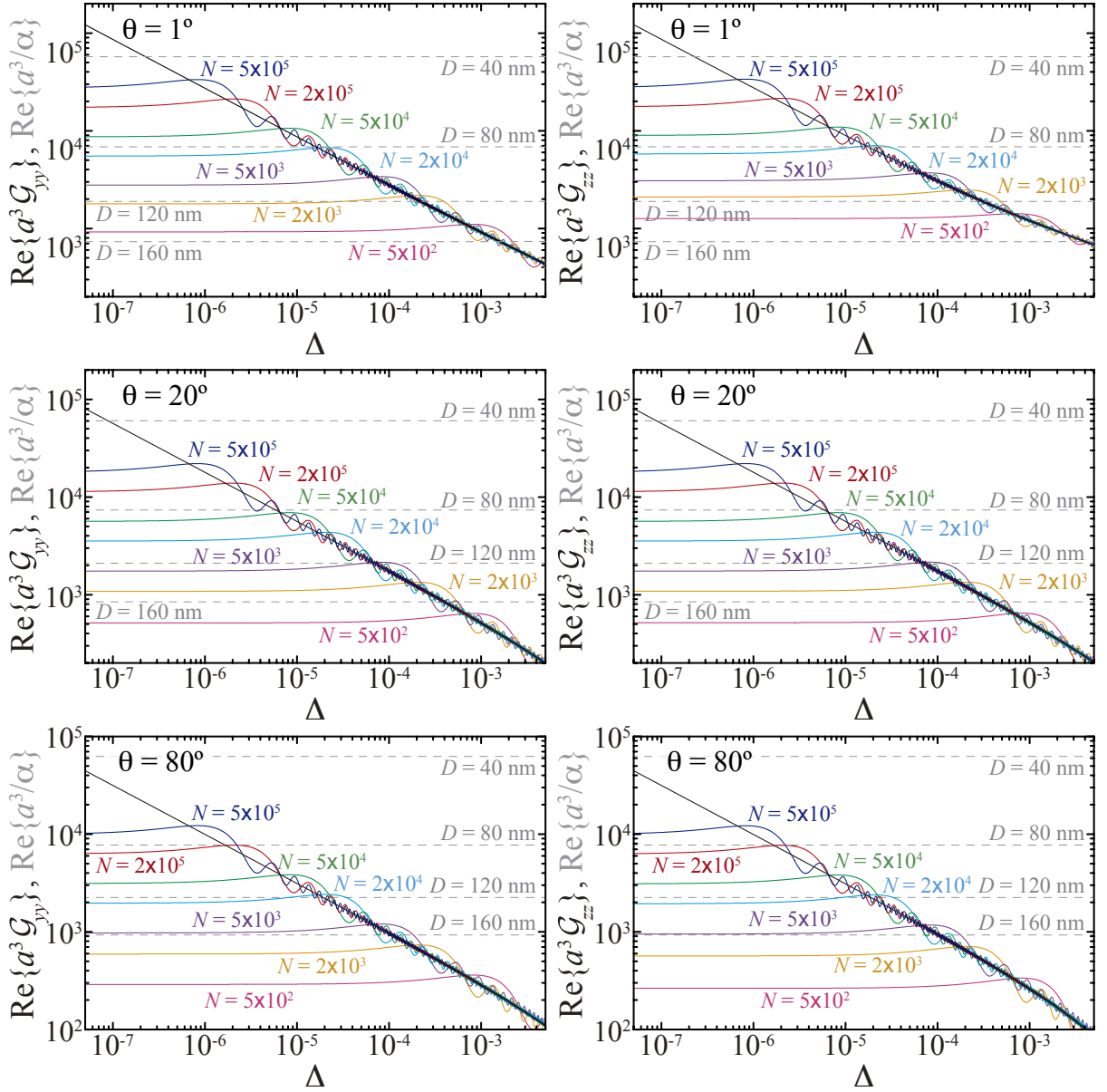


Figure S5: Finite-size effects on the lattice sum. Real part of the in-plane (*i.e.*, yy , left column) and the out-of-plane (*i.e.*, zz , right column) of the lattice sum calculated for different angles of incidence (black curve). The color curves represent the results obtained by truncating the lattice sum for an array of size $(N + 1) \times (N + 1)$, as described in the main paper (see Figure 5). The gray dashed lines indicate the real part of the inverse of the nanoparticle polarizability calculated for different values of D . In all cases, we assume $a = 800$ nm.

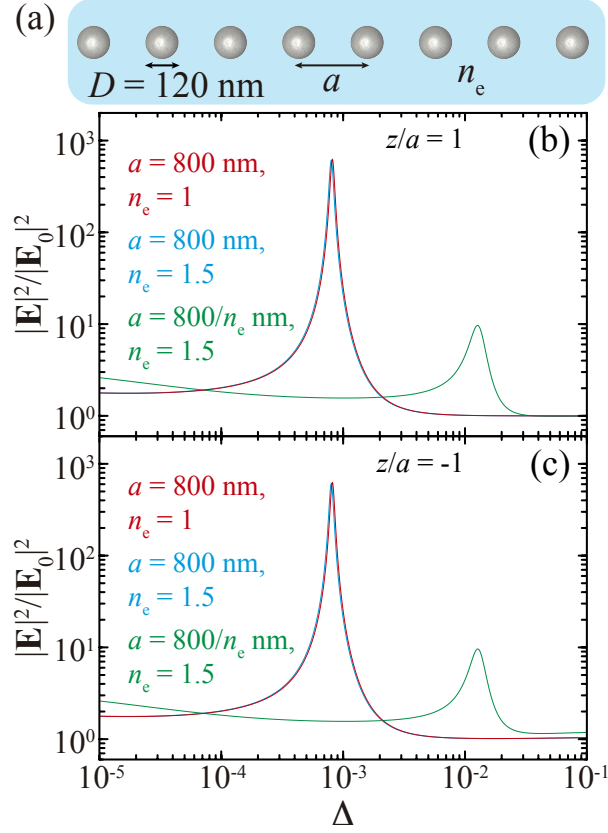


Figure S6: Analysis of the effect of a homogeneous dielectric environment. (a) Schematics of the system under consideration, consisting of an array of silver nanospheres of diameter $D = 120 \text{ nm}$ and periodicity a embedded in a medium of refractive index n_e . (b,c) Near-field intensity enhancement as a function of $\Delta = \lambda/(an_e) - 1$ for an array of periodicity $a = 800 \text{ nm}$ in vacuum (red curve) and in a medium with $n_e = 1.5$ (blue curve), as well as for an array with periodicity $a = 800/n_e \text{ nm}$ in a refractive index $n_e = 1.5$ (green curve). In panel (b), the field intensity enhancement is calculated at a height $z = a$ above the array, while, in panel (c), the calculation is done at $z = -a$. Examining these results, we observe that the near-field intensity enhancement produced by the two arrays with $a = 800 \text{ nm}$ are identical, and therefore the only effect of the change in the dielectric environment is a shift of the wavelength of the resonance (notice that now Δ depends on n_e). Such shift can be compensated by decreasing the array periodicity to $a = 800/n_e \text{ nm}$, however that results in an increase of the value of Δ of the lattice resonance and, therefore, in a reduction of the field enhancement produced by the array.

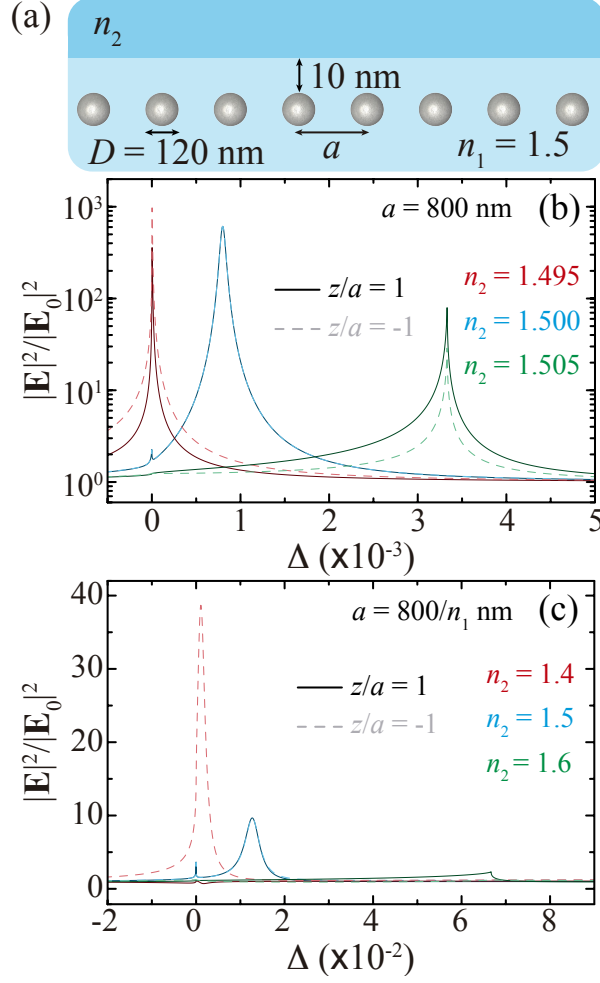


Figure S7: Analysis of the effect of an inhomogeneous dielectric environment. (a) Schematics of the system under consideration, consisting of an array of silver nanospheres of diameter $D = 120$ nm and periodicity a embedded in a medium of refractive index $n_1 = 1.5$ and situated a distance 10 nm from another medium with refractive index n_2 . As in the main paper, we assume light is incident from below the array (*i.e.*, from the side with n_1), which is located at $z = 0$. (b) Near-field intensity enhancement as a function of $\Delta = \lambda/(an_1) - 1$ for an array of periodicity $a = 800$ nm when $n_2 = 1.495$ (red curves), $n_2 = 1.5$ (blue curves), and $n_2 = 1.505$ (green curves). The dark solid curves correspond to the case in which the field is calculated at a distance $z/a = 1$ from the array, while the dashed lighter curves display the results for $z/a = -1$. (c) Same as (b), but for an array with periodicity $a = 800/n_1$ nm. In this case, the red, blue, and green curves correspond to $n_2 = 1.4$, $n_2 = 1.5$, and $n_2 = 1.6$, respectively. Examining the results of panel (b), we observe that, due to the large field enhancement, the system is very sensitive to asymmetries in the dielectric environment. When $n_2 < n_1$, the lattice resonance shifts to smaller Δ , which leads to an increase in the near-field enhancement, while, for $n_2 > n_1$, the resonance moves to larger values of Δ , thus leading to a decrease in the enhancement. On the other hand, systems producing smaller field enhancements, such as the array analyzed in panel (c), are less sensitive to asymmetric environments.

References

- (S1) García de Abajo, F. J.; Gómez-Medina, R.; Sáenz, J. J. Full Transmission Through Perfect-Conductor Subwavelength Hole Arrays. *Phys. Rev. E* **2005**, *72*, 016608.
- (S2) García de Abajo, F. J. Colloquium: Light Scattering by Particle and Hole Arrays. *Rev. Mod. Phys.* **2007**, *79*, 1267–1290.